PHYSICAL REVIEW D **79,** 045004 (2009)

Massless fermions in multiflavor QED_2

S. Nagy

Department of Theoretical Physics, University of Debrecen, Debrecen, Hungary

(Received 14 May 2008; published 4 February 2009)

The ground state of the multiflavor two-dimensional quantum electrodynamics is determined in the presence of finite baryon density, and it is shown that the model possesses two phases: the low-density phase where the external baryon density is totally screened, and the high-density phase where the screening is only partial. The renormalization of the bosonized version of the model is also performed for both the zero and the finite-density model giving massless multiflavor two-dimensional quantum electrodynamics in both cases.

DOI: 10.1103/PhysRevD.79.045004 PACS numbers: 11.10.Gh, 11.10.Hi, 11.10.Kk

I. INTRODUCTION

The phase structure and the confinement mechanism of non-Abelian models are usually investigated in much simpler, usually two-dimensional, ''toy'' models [1,2]. These models are sometimes analytically solvable. For example, the massless two-dimensional quantum electrodynamics (QED_2) [3] (usually referred to as the Schwinger model) shows the chiral condensate and a mass gap which are supposed to be essential elements in modern physics. The bosonized version of the Schwinger model is a free theory, which turns into interacting when the fermionic mass is nonzero [4]. QED_2 possesses a phase transition at $m/g_c \sim 0.31$ as was shown by the density matrix renormalization group (RG) technique [5] or by continuous RG method [6]. The critical value of m/g_c separates the large coupling ($g \gg m$) phase with a unique vacuum characterized by the field variable $\phi = 0$, and the weak coupling ($g \ll m$) phase where, due to spontaneously broken reflection symmetry, the model has nontrivial vacua at around $\phi = \pm\sqrt{\pi}/2$.

The ground state of quantum chromodynamics (QCD) occurs when a color superconductor at high densities [7] and a periodic chiral condensate appear in the coordinate space at a large number of colors N_c [8] which is recapitulated in the framework of RG equations by mapping QCD into a Thirring-type model [9]. The high-density behavior of non-Abelian models are investigated in the framework of toy models, too [10]. The Schwinger model remains exactly solvable in the presence of an external finite charge density and also shows periodic chiral condensate [11,12]. In our previous work [13] we showed that in the finite-density QED_2 the system exhibits a single periodic phase in the thermodynamic limit for arbitrary charge densities; furthermore, the periodic structure built up in the ground state has decreasing amplitude and wavelength with increasing charge density. It is assumed [2] that a phase transition appears in the two-flavor QED_2 as the density is increased. According to the bosonization technique [14] both the massless and the multiflavor QED_2 can be converted to such local scalar field theoretical models which contain periodic self-interaction potentials. The Bose form of the multiflavor QED_2 is a sine-Gordon–type scalar field theory [15–17], where periodic self-interactions are described by two-dimensional sine-Gordon (SG) fields which coupled by a mass matrix. This coupled SG [or layered sine-Gordon (LSG)] model can also be used to describe the vortex dynamics of magnetically coupled layered superconductors [18], where the number of flavors in the high-energy model is identical to the number of layers of the condensed matter system [17]. Moreover coupled SG-type models have been used to investigate the vortex dynamics of Josephson-coupled superconductors [19].

The phase transition of these models was obtained from the microscopic theory which is formulated in the high energy or ultraviolet (UV) region. In order to obtain the low energy or infrared (IR) physics, where the measurements are performed and the quantum fluctuations are taken into account, we need renormalization. The original, fermionic models, or the toy models, contain strong couplings and they disable performing a perturbative renormalization, making it rather difficult to develop a functional RG method in the fermionic models since the evolution should be started from a perturbative region where the theory is almost interaction-free. Furthermore the RG equations have to preserve the gauge symmetry [20]. However, the bosonized version of the toy models can be easily treated by the functional RG method [6,17,21].

Our goal in this article is to clarify the phase transition of the finite-density two-flavor QED_2 by the methods used in [13]. We calculate numerically (and also analytically in the low- and high-density limits) the ground state field configurations for finite external baryon density in the tree level. The results show that an induced baryon density appears which screens the external one totally (partially) for low (high) external baryon densities, respectively, showing the existence of two phases as is conjectured in [2]. We also perform the RG procedure to determine the IR physics of the zero and finite-density two-flavor QED_2 and then generalize the results for an arbitrary number of flavors. We choose the so-called Wegner-Houghton (WH) RG method [22] in order to obtain the blocked potential for

the model, which uses a gliding sharp cutoff k. The external baryon density produces coordinate dependent nontrivial saddle points, therefore we use the tree-level blocking relation [6,21,23] to get the blocked interaction potential. The RG evolution gives the flow of the couplings for the LSG model from which the evolution of the couplings of the fermionic model can be easily determined.

The paper is organized as follows. In Sec. II we show the connection between the fermionic and the bosonized models and then in Sec. III we determine the ground state field configuration of the finite-density two-flavor QED_2 and map its phase structure. We derive the evolution of the coupling in the framework of the WH-RG method in Sec. IV, and determine the flow of the couplings in the case of zero, low, and high densities. Finally, in Sec. V the conclusion is drawn up.

II. THE MODEL

The multiflavor QED_2 containing N Dirac fields with an identical fermionic charge e and a mass m has the Lagrangian density

$$\mathcal{L} = -\frac{1}{4}F_{\mu\nu}F^{\mu\nu} + \sum_{i=1}^{N}\bar{\psi}_i\gamma^\mu(\partial_\mu - ieA_\mu)\psi_i - m\sum_{i=1}^{N}\bar{\psi}_i\psi_i, \tag{1}$$

where $F_{01} = \partial_0 A_1 - \partial_1 A_0$. One can turn from fermionic field variables $\bar{\psi}_i$, ψ_i into bosonic ones ϕ_j by the bosonization rules [2,24]

$$\begin{aligned}
:\bar{\psi}_i\psi_i: &\to -cmM\cos(2\sqrt{\pi}\phi_i),\\
:\bar{\psi}_i\gamma_5\psi_i: &\to -cmM\sin(2\sqrt{\pi}\phi_i),\\
:\bar{\psi}_i\gamma_\mu\psi_i: &\to \frac{1}{\sqrt{\pi}}\varepsilon_{\mu\nu}\partial^\nu\phi_i,\\
:\bar{\psi}_i i\partial\!\!\!/\psi_i: &\to \frac{1}{2}N_m(\partial_\mu\phi_i)^2,
\end{aligned} \tag{2}$$

where N_m means normal ordering with respect to the fermion mass m, $M = e/\sqrt{\pi}$, and $c = \exp(\gamma)/2\pi$, with the Euler constant $\gamma = 0.5774$. The presence of a nonvanishing external or background densities does not affect these transformation rules [11]. The Hamiltonian of the system in Coulomb gauge is given by

$$\mathcal{H} = \sum_{i=1}^{N}\int_x \bar{\psi}_i(x)(i\gamma_1\partial_1 + m)\psi_i(x) - \frac{e^2}{4}\int_{x,y} j_{0,x}|x-y|j_{0,y}, \tag{3}$$

with $\int_x = \int_0^T dx^0 \int_{-L}^{L} dx^1$ and

$$j_{0,x} =: \sum_{i=1}^{N}\bar{\psi}_i(x)\psi_i(x) := \frac{1}{\sqrt{\pi}}\partial_1\sum_{i=1}^{N}\phi_i(x). \tag{4}$$

The resulting bosonized form of the Hamiltonian is

$$\mathcal{H} = N_m\int_x\Big[\frac{1}{2}\sum_{i=1}^{N}\Pi_i^2(x) + \frac{1}{2}\sum_{i=1}^{N}(\partial_1\phi_i(x))^2 + \frac{e^2}{2\pi}\times\Big(\sum_{i=1}^{N}\phi_i(x)\Big)^2 - cm^2\sum_{i=1}^{N}\cos(2\sqrt{\pi}\phi_i(x))\Big], \tag{5}$$

where $\Pi_i(x)$ denotes the momentum variable canonically conjugated to $\phi_i(x)$. Let us assume that the two distinct flavored fermion has the same mass m but opposite charge e. The resulting bosonic Hamiltonian corresponds to the LSG model

$$\mathcal{H} = N_M\int_x\Big[\frac{1}{2}\Pi_1^2 + \frac{1}{2}\Pi_2^2 + \frac{1}{2}(\partial_1\phi_1)^2 + \frac{1}{2}(\partial_1\phi_2)^2 + \frac{M^2}{2}(\phi_1-\phi_2)^2 - u(\cos(2\sqrt{\pi}\phi_1) + \cos(2\sqrt{\pi}\phi_2))\Big] \tag{6}$$

with two layers ($N = 2$), and $u = cme/\sqrt{\pi}$. The assumption for the charges corresponds to the situation where the net electric charge is zero, which means that the matter is colorless. It is assumed that this kind of colorless matter might exist in nuclear stars. Let us denote the two types of Bose field as ϕ_i with $i = 1, 2$. After introducing the new fields as

$$\phi_\pm = \frac{1}{\sqrt{2}}(\phi_1 \pm \phi_2), \tag{7}$$

the charge density $j_0 \equiv \rho$ and the baryon density B can be written as

$$\rho = \frac{2}{\sqrt{\pi}}\partial_1\phi_-, \qquad B = \frac{2}{\sqrt{\pi}}\partial_1\phi_+. \tag{8}$$

An external baryon charge density can be introduced by replacing ρ with $\rho + \rho_0$. If we define the corresponding classical potential as

$$\rho_0 = \frac{2}{\sqrt{\pi}}\partial_1\phi_c, \tag{9}$$

then the uniform, constant external baryon density is simply $\phi_c = bx$. We separate this linear term in the space direction $\phi_+ = \tilde{\phi}_+ + bx$, introduce the chemical potential μ, and assume that it is nonvanishing on the interval $[-L; L]$. Taking $b = -2\mu 2/\sqrt{\pi}$ then Hamiltonian reduces to

$$\mathcal{H} = N_M\int_x\Big[\frac{1}{2}\pi_-^2 + \frac{1}{2}(\partial_1\phi_-)^2 + M^2\phi_-^2 + \frac{1}{2}\pi_+^2 + \frac{1}{2}(\partial_1\tilde{\phi}_+)^2 - u'\cos(\sqrt{2\pi}\phi_-)\times\cos(\sqrt{2\pi}(\tilde{\phi}_+ + bx))\Big], \tag{10}$$

due to the normal ordering with respect to the bosonic mass M where the dimensionful coupling u',

$$u' = c' m^{3/2} e^{1/2}, \tag{11}$$

is introduced, and $c' = c(2/\pi)^{1/4}$. However, the periodic part of the Hamiltonian also gives a contribution to the mass spectrum, i.e. the normal ordering can also be defined with respect to the ''total'' mass. In this case the relation between the mass gap of the multiflavor bosonic model and the parameters of the original fermionic theory is

$$M_{\text{gap}} = 2.008 \cdot m^{N/(N+1)} e^{1/(N+1)}, \tag{12}$$

where N is the number of flavors [16]. The Hamiltonian (10) is a functional of the field configurations ϕ_- and ϕ_+, and it gives the energy of the system on the tree level. We look for the ground state field configuration of the model as the function of the density b.

III. THE TREE-LEVEL PHASE STRUCTURE

The minimum of the energy is searched numerically among the static field configurations, $\pi_\pm(x) = 0$ by means of conjugate gradient method as a function of the finite baryon density b. We made numerical calculations in order to minimize the tree-level energy as the functional of the field variables ϕ_- and ϕ_+. The results show that at the energy minimum $\phi_-(x) = 0$ for all values of b. This result is not surprising since in the Hamiltonian in Eq. (10) one has a massive sine-Gordon (MSG) model [1,2,24,25] with zero density for the field variable $\phi_-(x)$, and this model exhibits trivial field configurations on the tree-level approximation [13]. Therefore we can treat a simpler Hamiltonian

$$\mathcal{H} = \int_x \left[\frac{1}{2}\pi_+^2 + \frac{1}{2}(\partial_1 \tilde{\phi}_+)^2 - u' \cos(\sqrt{2\pi}(\tilde{\phi}_+ + bx)) \right], \tag{13}$$

which corresponds to a SG model [26] with finite density. Equation (13) leads to the equation of motion

$$(\partial_0^2 - \partial_1^2)\tilde{\phi}_+ + \sqrt{2\pi} u' \sin(\sqrt{2\pi}(\tilde{\phi}_+ + bx)) = 0. \tag{14}$$

Considering the static equation of motion and using a simple redefinition of the field variable, $\sqrt{2\pi}(\tilde{\phi}_+ + bx) \to \tilde{\phi}_+$ gives the static SG equation [27] which is identical to the evolution equation of a pendulum. Depending on the initial energy C of the pendulum, the model has two phases. When C is large, it makes periodic rotation corresponding to the kink (or antikink) crystal in the original model [27]. In the low-energy phase the pendulum swings, and we have a kink-antikink crystal. The external baryon charge contributes to the energy by the term πb^2. Then the large density limit corresponds to the kink-antikink crystal, while at low densities the kink crystal solution appears. The general analytic solution is

$$\tilde{\phi}_+ = -bx + \frac{1}{\sqrt{2\pi}} \text{am}\left(\frac{\sqrt{2\pi u'} x}{k}, r^2 \right) \tag{15}$$

with $\text{am}(x, r^2)$ the Jacobian elliptic function, and $r = \sqrt{2/(2 + C/2\pi u')}$. The coupling u' plays a key role in the RG procedure, so we keep it explicitly. We consider the limiting low density ($r \to \infty$ or small values of b) and high density ($r \to 0$ or high values of b) cases. The series representation of the function $\text{am}(x, r^2)$ is

$$\text{am}\,(x, r^2) = \frac{\pi x}{2K(r)} + 2 \sum_{n=1}^{\infty} \frac{q(r)^n}{n(q(r)^{2n} + 1)} \sin \frac{n\pi x}{K(r)}, \tag{16}$$

where $K(r)$ is the complete elliptic integral of the first kind and $q(r) = \exp(-\pi K(1 - r)/K(r))$. In the low-density limit $q(r) \to -1$ and the second term is just the Fourier expansion of the first term with opposite sign in the right-hand side of Eq. (16), giving $\text{am}(x, r^2) \to 0$, so

$$\tilde{\phi}_+ = -bx \tag{17}$$

as is conjectured in [2]. It gives a constant induced density equal to the external one with opposite sign, resulting total screening. At large densities the field configuration changes. When b is large $C \approx \pi b^2$ and the amplitude A_n of the nth Fourier expansion in Eq. (16) scales as $A_n \sim 1/b^{2n}$; therefore it is a good approximation to keep only the fundamental mode. Then the field configuration becomes

$$\tilde{\phi}_+ = -\frac{u'}{\sqrt{2\pi} b^2} \sin(\sqrt{2\pi} bx), \tag{18}$$

a sinusoidal-type one, giving sinusoidal induced density which only partially screens the external density, and the net baryon density turns to finite values signalling a phase transition going from low densities to high ones. In Fig. 1 two typical numerically obtained field configurations are plotted. The wavelength ℓ is insensitive for the fermion mass m, furthermore it decreases according to a power law in b for several orders of the density. The numerical fit gives that $\ell = \sqrt{2\pi}/b$ is equal to the ''specific volume'' of the external density similarly to the case of MSG model [13], as can be seen in Fig. 2. The amplitude A is a constant and independent of fermion mass for low densities since it is independent of the coupling u'. Because of the linear form of $\tilde{\phi}_+$ its value is $A = b\ell/2 = \sqrt{\pi/2}$. Going to a high-density regime the amplitude decreases as $A \sim 1/b^2$ and an m dependence appears. We plotted the amplitudes A_n in Fig. 3. The limiting low- and high-density cases are in good agreement with their analytically calculated value in Eqs. (17) and (18). Figure 3 shows that the phase transition appears around the critical value b_c. Using the field configurations obtained in Eqs. (17) and (18) one can calculate the total energy density $\mathcal{E}$ by inserting them back into Eq. (13). For low densities it is (l refers to *linear* field configurations)

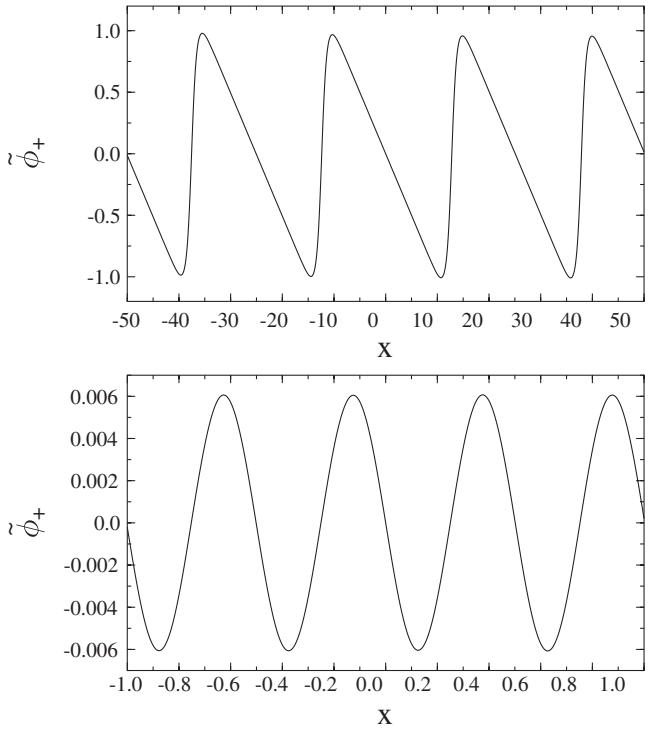

FIG. 1. The form of the field configuration for $b = 0.1$ (upper figure) and $b = 5$ (lower figure).

$$\mathcal{E}_l = \frac{b^2}{2} - u', \tag{19}$$

while in high densities one obtains (p refers to *periodic* field configurations)

$$\mathcal{E}_p = -\frac{u'^2}{4b^2}. \tag{20}$$

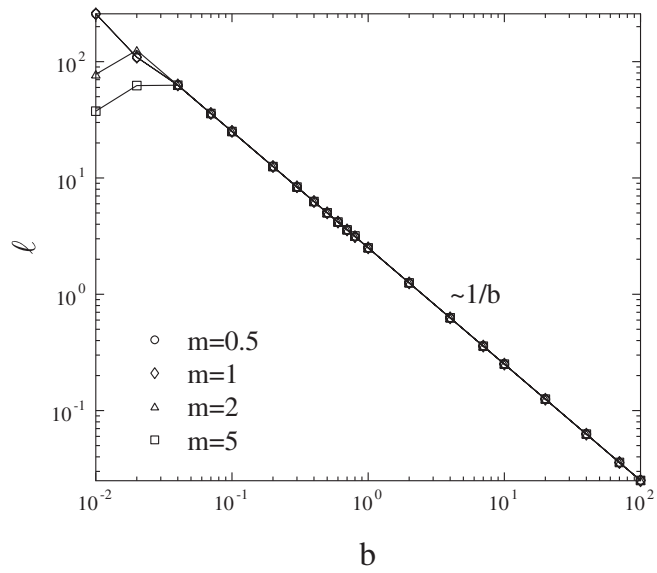

FIG. 2. The baryon density dependence of the wavelength ℓ of the field configuration $\tilde{\phi}_+$.

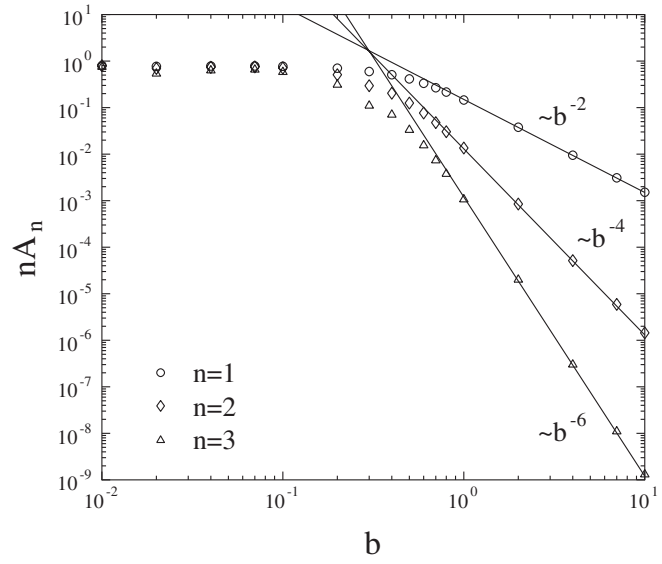

FIG. 3. The baryon density dependence of the Fourier modes A_n, $n = 1, 2, 3$. A_n follow a power law behavior at high densities as it was obtained analytically.

This shows that the energy density is always negative and the field configuration in Eq. (18) is energetically favorable in comparison with a trivial one which would give $\mathcal{E} = 0$. In Fig. 4 we plotted $\mathcal{E}_p$ and $\mathcal{E}_l$ and the numerically determined total energy density. At low densities the linear field configuration is preferable and the sinusoidal one is preferred for high densities. The high-density phase then contains a coordinate dependent ground state which is supposed to flatten out when one takes into account the

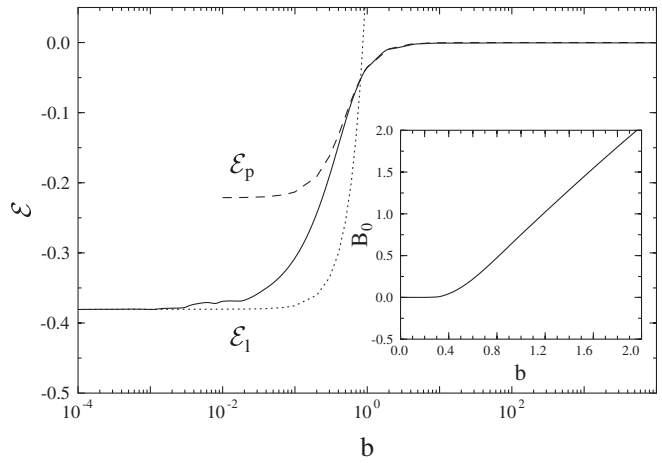

FIG. 4. The baryon density dependence of the energy density in case of linear $\mathcal{E}_l$ (dotted line) and periodic $\mathcal{E}_p$ (dashed line) configurations. We also plotted the numerically determined total energy density by a solid line. The numerical results coincide with the linear field configuration at low densities and with the periodic field configuration at high densities. The inset shows how the baryon density B_0 increases as the background baryon density b grows.

quantum fluctuations beyond the tree-level approximation [2]. The critical density b_c which separates the low- and the high-density phases can be read off correctly from Fig. 3 as the intersection of the Fourier modes, which is $b_c \approx 0.3$. The baryon density at the origin $B(x=0) \equiv B_0$ can play the role of the order parameter of the phase transition. It is zero in the low-density phase and is finite in the high one, as can be seen in the inset of Fig. 4. According to the inset of Fig. 4 the phase transition seems a continuous one.

IV. RENORMALIZATION

The phase structure of the finite-density two-flavor QED$_2$ is determined at the tree level where the observational scale k is in the UV regime. We use the RG method to lower the scale k into the IR limit in order to consider the effect of the quantum fluctuations systematically. Here we perform the RG treatment of the LSG model for zero, and then for finite density. We treat the model in a more general form containing the arbitrary frequency parameter β. The bosonization works for the specific choice $\beta^2 = 4\pi$, gives the Hamiltonian in Eq. (6), and in this article we map the phase structure as the function of the baryon density b. However, the phase structure can be also considered in terms of the frequency β with the critical value $\beta_c^2 = 16\pi$ in the LSG model [28]. At the scale where the microscopic theory is formulated the local potential approximation is usually valid, implying that during the blocking transformation a constant field configuration gives the minimum of the potential [22,29]; furthermore, the RG methods based on the evolution of the effective action [30] are also formulated with constant field configurations. We showed in the preceding section that for the finite-density two-flavor QED$_2$ it is not the case. The nontrivial saddle point field configuration makes unstable modes, and one should take into account coordinate dependent field configuration to find the real extremum of the Lagrangian, or at least better than the constant field configuration could give [23,31]. Therefore we choose the WH-RG method where one can change to tree-level blocking relation when the nontrivial saddle point appears [23]. In this RG method the blocked potential can be derived by means of the differential RG in momentum space at the gliding momentum scale $k \in [0, \Lambda]$. In the WH-RG approach the field fluctuations are ordered by their decreasing frequencies and during the blocking step one integrates out the high-frequency modes above the cutoff k, keeping the generating functional invariant. We decompose the field variables into the high-frequency $\phi'_x = \int_{|p|>k} \phi_p e^{ipx}$ and the low-frequency $\phi_x = \int_{0\le|p|\le k} \phi_p e^{ipx}$ modes. The high-frequency modes are integrated out step by step in infinitesimal momentum shells of thickness Δk,

$$e^{-S_{k-\delta\Delta k}[\phi]} = \int \mathcal{D}[\phi'] e^{-S_k[\phi+\phi']}, \tag{21}$$

with $S_k[\phi]$ the blocked action in Euclidean spacetime. The higher frequency Fourier modes are split further into the sum of the saddle point field configuration ϕ^{sp} and the remaining field fluctuations: $\phi' = \phi^{\mathrm{sp}} + \varphi$. In order to evaluate the blocked action in Eq. (21), we expand the blocked action in the Taylor series around its saddle point field configuration. Then, for trivial saddle points $\phi^{\mathrm{sp}} = 0$ one arrives at the WH-RG equation [28]

$$(2 + k\partial_k)\tilde{V}_k = -\frac{1}{4\pi}\log((1+\tilde{V}_k^{11})(1+\tilde{V}_k^{22}) - (\tilde{V}_k^{12})^2), \tag{22}$$

for the LSG model with $N = 2$ and the second derivatives $\tilde{V}_k^{ij} = \partial_{\phi_i}\partial_{\phi_j}\tilde{V}_k$ (all dimensionless quantities are denoted by a tilde superscript), which is introduced as the sum of the dimensionless mass term and the dimensionless periodic potential,

$$\tilde{V}_k(\phi_1, \phi_2) = \tilde{M}(\phi_1 - \phi_2)^2 + \tilde{U}_k(\phi_1, \phi_2), \tag{23}$$

which is the generalized Euclidean form of the Hamiltonian in Eq. (6). The ansatz for the periodic part of the potential is

$$\tilde{U}_k = \sum_{n_1,n_2} [\tilde{u}_{n_1n_2}\cos(n_1\beta\phi_1)\cos(n_2\beta\phi_2) + \tilde{v}_{n_1n_2}\sin(n_1\beta\phi_1)\sin(n_2\beta\phi_2)]. \tag{24}$$

The scale dependence is entirely encoded in the dimensionless couplings $\tilde{u}_{n_1n_2} = u_{n_1n_2}/k^2$ and $\tilde{v}_{n_1n_2} = v_{n_1n_2}/k^2$. By inserting Eq. (23) into the functional evolution equation in Eq. (22) and Fourier expanding it, we obtain a set of coupled differential equations for these couplings. The right-hand side of the WH-RG equation in Eq. (22) turns out to be periodic, while the left-hand side contains periodic and nonperiodic parts, as well. Separating them, we obtain a trivial evolution,

$$\tilde{M}_k = \tilde{M}_\Lambda\left(\frac{k}{\Lambda}\right)^{-2}, \tag{25}$$

hence the dimensionful bosonic mass M_k remains constant during the RG procedure. We note that the RG flow equation in Eq. (22) keeps the periodicity of the periodic piece $\tilde{U}_k$ of the blocked potential in both directions of the internal space with unaltered length of periods, therefore β does not evolve in the local potential approximation.

During the successive integrations of the higher momentum modes of Eq. (22) by the method of steepest descent, it is assumed that the saddle points $(\phi_1^{\mathrm{sp}}, \phi_2^{\mathrm{sp}})$ are zero. It remains trivial until the second functional derivative of the blocked action S_k'' [the argument of the logarithm in Eq. (22)] is positive definite. When

$$S_k'' = (1+\tilde{V}_k^{11})(1+\tilde{V}_k^{22}) - (\tilde{V}_k^{12})^2) = 0, \tag{26}$$

the restoring force for the field fluctuations with momenta in the momentum shell $k - \Delta k < |p| < k$ vanish, i.e. their amplitudes can grow to finite values, and ϕ^{sp} becomes

nonvanishing, and the spinodal instability appears. Then, the tree-level blocking relation is needed [6,21,23,32]

$$S_{k-\Delta k}[\phi_1, \phi_2] = \min_{\phi_1^{\rm sp}, \phi_2^{\rm sp}} (S_k[\phi_1 + \phi_1^{\rm sp}, \phi_2 + \phi_2^{\rm sp}]). \quad (27)$$

In case of two layers the exchange of the field variables is a symmetry of the model, therefore the saddle point can be considered the same for both fields, namely,

$$\phi_1^{\rm sp} = \phi_2^{\rm sp} \equiv \phi^{\rm sp} = 2\rho_k \cos(kx^1). \quad (28)$$

It is assumed that the periodic coordinate dependence appears only in the space direction, which suits well to the treatment of the inhomogeneous ground states. Restricting ourselves to a finite interval $[-L; L]$ there is a periodic boundary condition for the saddle point, $\phi^{\rm sp}(x - L) = \phi^{\rm sp}(x + L)$. Then the tree-level blocking for the boson mass M_k has the form

$$M_{k-\Delta k}(\phi_0^1 - \phi_0^2)^2 = M_k(\phi_0^1 - \phi_0^2)^2 \rightarrow k\partial_k M_k = 0. \quad (29)$$

So $M_k \equiv M$ is a constant in the case of tree-level blocking as well. Thus, $\tilde{M}_k \sim k^{-2}$ is a relevant coupling for all scales. The blocking step

$$V_{k-\Delta k}[\phi_1^0, \phi_2^0] = \min_{\rho_k}\Big[2\rho_k k^2 + \sum_{n_1,n_2}[(u_{n_1n_2} + v_{n_1n_2}) \times \cos(\beta(n_1\phi_1^0 - n_2\phi_2^0))(2(n_1 - n_2) \times \beta\rho_k) + (u_{n_1n_2} - v_{n_1n_2})\cos(\beta(n_1\phi_1^0 + n_2\phi_2^0))(2(n_1 + n_2)\beta\rho_k)]\Big] \quad (30)$$

determines the tree-level evolution for the couplings. The SG and the MSG models showed that the phases of these models can be distinguished by the appearance of the spinodal instability [6,21]. Since only the fundamental mode is relevant both in the SG and the MSG models, perhaps it is not so surprising that the condition of spinodal instability gave a very good approximation for a single coupling. Close to the scale of spinodal instability $k_{\rm SI}$ the effective potential starts to form a parabolic shape [21], so the minimum of the blocked potential is situated always at the values of the field variables $\phi_1 = \phi_2 = 0$. Taking into account the first few couplings ($\tilde{u}_{01}$, $\tilde{u}_{11}$, and $\tilde{v}_{11}$) and inserting it into Eq. (26), one obtains

$$(1 + 2\tilde{M}_k - \tilde{u}_{01}\beta^2 - \tilde{u}_{11}\beta^2 - \tilde{v}_{11}\beta^2) \times (1 - \tilde{u}_{01}\beta^2 - \tilde{u}_{11}\beta^2 + \tilde{v}_{11}\beta^2) = 0. \quad (31)$$

The fundamental mode follows the scaling relation

$$\tilde{u}_{01} = \tilde{u}_{01}(\Lambda)\left(\frac{k^2 + 2M}{\Lambda^2 + 2M}\right)^{\beta^2/16\pi}\left(\frac{k}{\Lambda}\right)^{-2+\beta^2/8\pi}. \quad (32)$$

The scale $k_{\rm SI}$ can be situated below or above the mass scale M, so one can distinguish two cases:

(1) $k_{\rm SI} < M$. The results of the Appendix show $\tilde{u}_{11} = \tilde{v}_{11}$ (the massive modes) and Eq. (31) reduces to

$$(1 + 2\tilde{M}_k - \tilde{u}_{01}\beta^2 - 2\tilde{u}_{11}\beta^2)(1 - \tilde{u}_{01}\beta^2) = 0. \quad (33)$$

The expression cannot be zero if $\beta^2 > \beta_c^2$ since $\tilde{u}_{01}$ is irrelevant. If $\beta^2 < \beta_c^2$ then the expression $1 - \tilde{u}_{01}\beta^2$ will always go below zero, because now $\tilde{u}_{01}$ is relevant and grows up.

(2) $k_{\rm SI} > M$. Then the massive modes are irrelevant keeping their UV scaling according to Eq. (32) but the coupling $\tilde{u}_{01}$ scales relevantly when $\beta^2 < \beta_c^2$, which implies that the expression in the second parenthesis in Eq. (31) can be negative. When $\beta^2 > \beta_c^2$, then there is no spinodal instability.

The discussion gives that the critical value of β changes as compared to the case of the SG model, now $\beta_c^2 = 16\pi$. Since in our model $\beta^2 = 4\pi$ the spinodal instability always occurs. It was shown [33] that in this phase the couplings $\tilde{u}_{n_1n_2}$ are relevant at least in the UV region.

We have taken into account eight couplings when we solved the evolution equations numerically. As in [6,21] we obtained that the higher modes do not affect the scaling of the fundamental mode. However, the other couplings flow by different scaling behavior as obtained by an extended UV RG approach [17,33]. We started the evolution with the WH-RG method then at the scale $k_{\rm SI}$ we turned to the tree-level blocking equations. In the region $\beta^2 > \beta_c^2$ a very interesting scaling law appears, as shown in the Appendix. Furthermore, when $\beta^2 = 4\pi$ we run into the region of spinodal instability. The numerical results can be seen in Fig. 5. We numerically obtain that the dimensionless fundamental mode goes to a constant as in [21] independently of the relation between $k_{\rm SI}$ and M, and the IR value of $\tilde{u}_{01}(0)$ is superuniversal, independent of any UV parameter. When $k_{\rm SI} < M$ the flow of the fundamental mode qualitatively changes as the scale k goes below M. From Eq. (32) one obtains $\tilde{u}_{01}(k \rightarrow \infty) \sim k^{-1}$ in the UV limit but well below the mass scale M when $k^2 \ll 2M^2$ the flow scales according to $\tilde{u}_{01}(k \ll M) \sim k^{-3/2}$, and after we reach the scale $k_{\rm SI}$ and go towards the IR regime the flow runs into $\tilde{u}_{01}(0)$. The evolution is similar in the case of $k_{\rm SI} > M$, but since the tree-level blocking relation in Eq. (30) is independent of M, then below M the scaling cannot change. Because of the necessity of the double Fourier expansion we are unable to get as reliable numerical data as in [21], and we cannot read off the IR form of the effective potential. From the solution of the condition $S_k'' = 0$ [6,21] and the qualitative value of $\tilde{u}_{01}(0) \approx 0.14$ one expects

$$\tilde{V}_{k\rightarrow 0} = -\frac{1}{2}(\phi_1^2 + \phi_2^2). \quad (34)$$

The IR physics of the zero density LSG model is free, the dimensionful coupling vanishes as $k \rightarrow 0$ at $\beta^2 = 4\pi$.

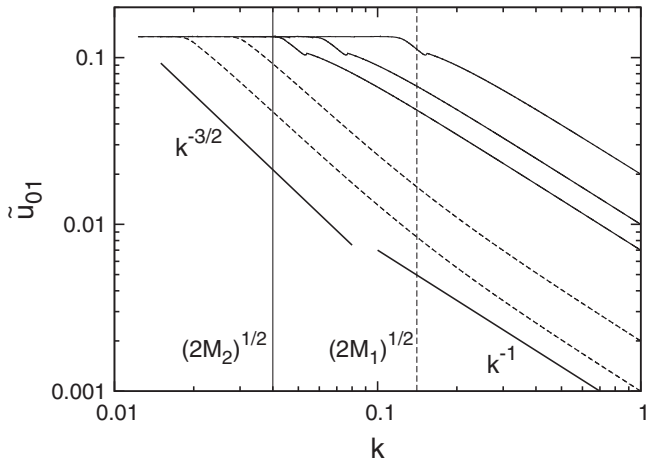

FIG. 5. The scaling of the fundamental mode $\tilde{u}_{01}$ for two different values of bosonic mass, $M_1 = 0.141$ (dashed lines) and $M_2 = 0.04$ (solid lines). For M_1 the UV (k^{-1}) and the IR ($k^{-3/2}$) scaling laws are drawn as reference.

However, there are two phases with the critical value β_c^2 and they can be distinguished by the different scaling behavior of the dimensionful couplings; namely, when $\beta^2 < \beta_c^2$, then the coupling scales as $u_{01} \sim k^2$, while in the case of $\beta^2 > \beta_c^2$ the scaling relation is $u_{01} \sim k^{\beta^2/8\pi}$. Nevertheless according to the flow of the dimensionless couplings, in the phase $\beta^2 < \beta_c^2$ the fundamental mode goes to a constant value, so it is marginal but in the other phase it vanishes; therefore it is irrelevant in the IR limit.

A. Massless fermions in multiflavor QED$_2$

One can easily generalize the previous analysis for multiflavor systems. We note that the critical value is $\beta_c^2 = 8\pi N/(N-1)$ [17], so the spinodal instability always appears at $\beta^2 = 4\pi$. The results of the RG analysis can be easily generalized and can show that the dimensionless coupling $\tilde{u}_k$ tends to constant values in the IR limit. Transforming the couplings of the scalar model (u_k and M_k) into the fermionic ones (g_k and m_k) one has

$$M_k^2 = \frac{e_k^2}{\pi}, \qquad u_k = \frac{e^\gamma}{2}\pi^{-(2N+1)/2N} m^{(2N-1)/N} e^{1/N}. \quad (35)$$

The dimensionful minimal coupling e_k does not scale independently of N, therefore the fermionic mass m_k should follow the irrelevant scaling of u_k

$$m_{k\to 0} \sim k^{2[N/(2N-1)]} \to 0, \quad (36)$$

meaning that in the IR limit we always have massless multiflavor QED$_2$. The pure QED$_2$ with $N = 1$ is not massless, since the tree-level blocking gives trivial (which is relevant in $d = 2$) scaling for the dimensionless coupling $\tilde{u}_k$. Therefore the fermionic mass becomes constant, showing that the cases $N = 1$ and $N \neq 1$ significantly differs [15,17].

1. Low-density phase

Now let us turn to the case when $b \neq 0$. The renormalization is rather involved in finite-density systems due to the coordinate dependent ground state field configurations. However in the low-density phase average baryon density is zero (the low external baryon density is totally screened by the induced density), and the resulting Hamiltonian becomes the same as in the zero density case. Therefore we look for the RG evolution of the model eventually among constant field configurations just in the case of $b = 0$, so all the results obtained there are valid in this phase too. It implies that the low-density LSG model is free, the fundamental mode is marginal, and the dimensionful coupling scales as $u_{01} \sim k^2$. The corresponding low-density two-flavor QED$_2$ is massless in the IR limit.

2. High-density phase

We consider the RG evolution only for the high-density limit. Here we always have a nontrivial saddle point $\phi^{\rm sp}$, and the quantum fluctuations take place around this field configuration. However, during the blocking steps $\phi^{\rm sp}$ also changes, which contributes to the evolution of order $\mathcal{O}(\hbar^0)$, therefore we concentrate on the evolution only of the $\phi^{\rm sp}$. Using the tree-level blocking relation in Eq. (27), one obtains

$$\begin{aligned} S_{k-\Delta k}[\phi] &= u'_{k-\Delta k}\frac{1}{b}\sqrt{\frac{2}{\pi}}\cos(\sqrt{2\pi}\phi)\sin(\sqrt{2\pi}bL) \\ &= \int_x \Big[\frac{1}{2}(\partial_1\phi^{\rm sp})^2 \\ &\quad + u'_k\cos(\sqrt{2\pi}(\phi+\phi^{\rm sp}+bx))\Big], \end{aligned} \quad (37)$$

with ϕ a constant field configuration. In the high-density limit the amplitude A_1 is small and can be considered perturbatively. Furthermore at high densities one can retain only the fundamental mode. Then the numerically determined form of the saddle point field configuration is

$$\phi^{\rm sp} = -A_1\sin(\sqrt{2\pi}(bx+\phi)) + A_1\sin(\sqrt{2\pi}\phi), \quad (38)$$

with $A_1 = u'_k/\sqrt{2\pi}b^2$. After identifying the corresponding functionals in Eq. (38) one obtains

$$u'_{k-\Delta k} = u'_k\Big(1 - \frac{u'^2_k}{4b^4}\Big) \quad (39)$$

for the infinitesimal blocking step. The blocking relation in Eq. (39) clearly shows that dimensionful coupling u'_k decreases, and tends to zero so as the amplitude A_1. Since the ratio $\Delta k/k$ is kept small in the WH-RG procedure, the blocking relation in Eq. (39) is valid for the dimensionless couplings too, implying that the fundamental mode is irrelevant in the high-density phase. The quantum fluctuations really wash out the wavy field configurations, although at that price that in the IR limit one obtains a

free theory in the high-density phase, too, so the high-density two-flavor QED_2 is also massless.

V. CONCLUSIONS

We determined the phase structure of the bosonized version of the two-flavor QED_2 and showed that in the tree level the induced baryon density totally screens the low external baryon density b. In the case of high densities the screening is only partial; furthermore, a wavy induced baryon density is obtained. We also performed the renormalization of the bosonized model in both phases. When b is zero then during the evolution a nontrivial saddle point appears and the tree-level blocking gives a dimensionful periodic potential which flattens out, implying massless two-flavor QED_2 in the IR limit. It is also the case when b is small, since there is a total screening and the model becomes similar to that of the zero density one. The evolution of the bosonized model in the high-density phase shows that the amplitude A of the periodic field configuration decreases as the quantum fluctuations are integrated out step by step as is the fermionic mass, and in the IR limit we obtain a massless theory with a trivial ground state. The scaling of the dimensionless fundamental mode is marginal in the low density and irrelevant in the high-density phases in the bosonized model; therefore, the phases found at the tree level survive the RG evolution and exist in the IR limit.

ACKNOWLEDGMENTS

The author acknowledges support from the Grant Öveges of the National Office for Research and Technology, and the Grant of Universitas Foundation, Debrecen.

APPENDIX A: IRRELEVANT RENORMALIZABLE OPERATOR IN THE LSG MODEL

The evolution equation will generate the higher order Fourier modes, so one should take them into account according to the ansatz in Eq. (24). We introduce a truncation in the number of couplings, namely $n_1, n_2 \leq 2$. Then we have eight apparently independent Fourier modes. The dimensionless WH-RG equation is

$$(2 + k\partial_k)\tilde{U}_k = -\alpha \log[(1 + 2\tilde{M}_k) + (1 + \tilde{M}_k)(\tilde{U}_k^{11} + \tilde{U}_k^{22}) + \tilde{U}_k^{11}\tilde{U}_k^{22} + 2\tilde{U}_k^{12}\tilde{M}_k - (\tilde{U}_k^{12})^2]. \quad \text{(A1)}$$

Now one has to Fourier expand the equation to get the evolution equation for the couplings. The resulting system of the ordinary differential equation is tackled by a numerical program. As we mentioned, the RG flow always runs into the spinodal instability when $\beta^2 < \beta_c^2$. In Fig. 6 one can see the typical IR flow of the couplings. One can reach the following conclusions from the numerical analysis:

(1) We numerically obtained that instead of eight couplings we have only five independent ones, $\tilde{u}_{11}(k \to 0) = \tilde{v}_{11}(k \to 0)$, $\tilde{u}_{12}(k \to 0) = \tilde{v}_{12}(k \to 0)$, and $\tilde{u}_{22}(k \to 0) = \tilde{v}_{22}(k \to 0)$, implying that the ansatz of the periodic part of the potential in Eq. (23) can be simply taken as

$$\tilde{V}_k = \frac{1}{2}M(\phi_1 - \phi_2)^2 + \sum_{n_1,n_2=0}^{\infty} \tilde{u}_{n_1 n_2} \times \cos(n_1\beta\phi_1 - n_2\beta\phi_2). \quad \text{(A2)}$$

This result is independent of the value of β.

(2) At the scale around the mass of the theory $\sim\sqrt{\tilde{M}_k}$ the scaling of the couplings change. There are modes which scale trivially below $\sqrt{\tilde{M}_k}$, namely,

$$\tilde{u}_{n_1 n_1} \sim k^{-2}, \quad \text{(A3)}$$

and they are referred as massive modes. Furthermore the other modes have qualitatively new scaling behavior. Numerical results show that in general the Fourier amplitudes scales according to the law

$$\tilde{u}_{n_1 n_2} \sim k^{|n_1 - n_2|[(\beta^2/8\pi)-2]-2\delta_{n_1,n_2}}, \quad \text{(A4)}$$

with the Kronecker delta $\delta_{x,y}$. This result is also valid for arbitrary value of β, but when $\beta < \beta_c$ the Eqs. (A3) and (A4) are correct until $k > k_{SI}$. Below the scale of the spinodal instability the scaling relations of the flow changes.

(3) Starting from different UV initial values of the Fourier modes one obtains that only the fundamental mode $\tilde{u}_{01}$ is sensitive for the initial conditions. The sensitivity matrix has the same structure as in

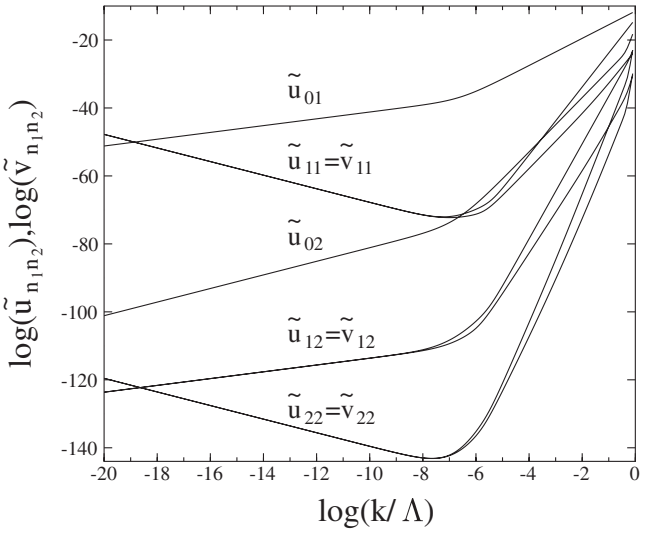

FIG. 6. For $\beta^2 = 24\pi$ the IR behavior of various Fourier amplitudes is presented for the LSG model.

the case of the SG and MSG models [6,21] where the matrix has only one nonzero column. We numerically obtained that the quantity

$$\frac{\tilde{u}_{n_1 n_2}(k \to 0)}{\tilde{u}_{01}^{n_1+n_2}(\Lambda)} \equiv c_{n_1 n_2}(k) \tag{A5}$$

is independent of $\tilde{u}_{n_1 n_2}(\Lambda)$ and $\tilde{v}_{n_1 n_2}(\Lambda)$. Consequently, according to the sensitivity matrix the only relevant operator is the fundamental mode $\tilde{u}_{01}$ which drives the IR behavior of all the other couplings. On the other hand, according to the scaling law in Eq. (A4) $\tilde{u}_{01} \sim k^{\beta^2/8\pi-2}$ with positive exponent in the case of $\beta > \beta_c$ giving an irrelevant scaling.

By the numerical solution of the RG equation derived for the LSG model we show that for $\beta > \beta_c$ one can parametrize the RG flow of the couplings by the initial value of the fundamental mode $\tilde{u}_{01}(\Lambda)$, including the IR relevant massive modes. The results of the sensitivity matrix show that the fundamental mode is the only relevant operator of the model; nevertheless it goes to zero, so according to common classification of the couplings it is irrelevant. Therefore, the scaling of all the higher harmonics and hence the low energy effective theory of the LSG model is driven by an irrelevant coupling, showing the essential importance of the investigation of irrelevant operators and the RG technique.

[1] S. Coleman, R. Jackiw, and L. Susskind, Ann. Phys. (N.Y.) **93**, 267 (1975); H. J. Rothe, K. D. Rothe, and J. A. Swieca, Phys. Rev. D **19**, 3020 (1979).

[2] W. Fischler, J. Kogut, and L. Susskind, Phys. Rev. D **19**, 1188 (1979).

[3] J. Schwinger, Phys. Rev. **125**, 397 (1962); **128**, 2425 (1962); J. H. Lowenstein and J. A. Swieca, Ann. Phys. (N.Y.) **68**, 172 (1971); A. Casher, J. Kogut, and L. Susskind, Phys. Rev. D **10**, 732 (1974).

[4] C. Adam, Ann. Phys. (N.Y.) **259**, 1 (1997); Phys. Lett. B **394**, 161 (1997); **555**, 132 (2003).

[5] T. M. R. Byrnes, P. Sriganesh, R. J. Bursill, and C. J. Hamer, Nucl. Phys. B, Proc. Suppl. A **109**, 202 (2002); Phys. Rev. D **66**, 013002 (2002).

[6] S. Nagy, I. Nandori, J. Polonyi, and K. Sailer, Phys. Rev. D **77**, 025026 (2008).

[7] D. Bailin and A. Love, Phys. Rep. **107**, 325 (1984); B.-Y. Park, M. Rho, A. Wirzba, and I. Zahed, Phys. Rev. D **62**, 034015 (2000); R. Rapp, T. Schäfer, E. V. Shuryak, and M. Velkovsky, Phys. Rev. Lett. **81**, 53 (1998).

[8] D. V. Deryagin, D. Yu. Grigoriev, and V. A. Rubakov, Int. J. Mod. Phys. A **7**, 659 (1992).

[9] E. Shuster and D. T. Son, Nucl. Phys. **B573**, 434 (2000).

[10] H. R. Christiansen and F. A. Schaposnik, Phys. Rev. D **53**, 3260 (1996); **55**, 4920 (1997); V. Schön and M. Thies, Phys. Rev. D **62**, 096002 (2000); M. Thies, Phys. Rev. D **69**, 067703 (2004).

[11] Y.-C. Kao and Y.-W. Lee, Phys. Rev. D **50**, 1165 (1994).

[12] M. A. Metlitski, Phys. Rev. D **75**, 045004 (2007).

[13] S. Nagy, J. Polonyi, and K. Sailer, Phys. Rev. D **70**, 105023 (2004).

[14] J. von Delft and H. Schoeller, Ann. Phys. (Leipzig) **7**, 225 (1998).

[15] J. E. Hetrick, Y. Hosotani, and S. Iso, Phys. Lett. B **350**, 92 (1995); Phys. Rev. D **53**, 7255 (1996); R. Rodriguez and Y. Hosotani, Phys. Lett. B **375**, 273 (1996); Y. Hosotani and R. Rodriguez, J. Phys. A **31**, 9925 (1998).

[16] A. V. Smilga, Phys. Rev. D **55**, R443 (1997).

[17] I. Nandori, Phys. Lett. B **662**, 302 (2008).

[18] I. Nandori, K. Vad, S. Meszaros, U. D. Jentschura, S. Nagy, and K. Sailer, J. Phys. Condens. Matter **19**, 496 211 (2007); **19**, 236 226 (2007).

[19] L. Benfatto, C. Castellani, and T. Giamarchi, Phys. Rev. Lett. **98**, 117008 (2007); **99**, 207002 (2007); A. N. Artemov, arXiv:0708.2775.

[20] M. Reuter and C. Wetterich, Nucl. Phys. **B391**, 147 (1993); J. Alexandre, J. Polonyi, and K. Sailer, Phys. Lett. B **531**, 316 (2002); T. R. Morris and Oliver J. Rosten, J. Phys. A **39**, 11 657 (2006); S. Arnone, T. R. Morris, and O. J. Rosten, Eur. Phys. J. C **50**, 467 (2007).

[21] S. Nagy, I. Nandori, J. Polonyi, and K. Sailer, Phys. Lett. B **647**, 152 (2007).

[22] F. J. Wegner and A. Houghton, Phys. Rev. A **8**, 401 (1973); K. G. Wilson and J. Kogut, Phys. Rep. **12C**, 75 (1974); K. G. Wilson, Rev. Mod. Phys. **47**, 773 (1975); Rev. Mod. Phys. **55**, 583 (1983); I. Nandori, J. Polonyi, and K. Sailer, Phys. Rev. D **63**, 045022 (2001); I. Nandori, J. Polonyi, and K. Sailer, Philos. Mag. B **81**, 1615 (2001); I. Nandori, U. D. Jentschura, K. Sailer, and G. Soff, Phys. Rev. D **69**, 025004 (2004).

[23] J. Alexandre, V. Branchina, and J. Polonyi, Phys. Lett. B **445**, 351 (1999); J. Polonyi, arXiv:hep-th/0509078.

[24] S. Coleman, Ann. Phys. (N.Y.) **101**, 239 (1976).

[25] I. Ichinose and H. Mukaida, Int. J. Mod. Phys. A **9**, 1043 (1994); Wen-Fa Lu, Phys. Rev. D **59**, 105021 (1999); S. W. Pierson and O. T. Valls, Phys. Rev. B **61**, 663 (2000); S. Nagy, J. Polonyi, and K. Sailer, J. Phys. A **39**, 8105 (2006).

[26] S. R. Coleman, Phys. Rev. D **11**, 2088 (1975); D. J. Amit, Y. Y. Goldschmidt, and G. Grinstein, J. Phys. A **13**, 585 (1980); J. Balog and A. Hegedus, J. Phys. A **33**, 6543 (2000); M. Faber and A. N. Ivanov, Eur. Phys. J. C **20**, 723 (2001); G. Takacs and F. Wagner, Nucl. Phys. **B741**, 353 (2006).

[27] W. L. McMillan, Phys. Rev. B **16**, 4655 (1977); G. Theodorou and T. M. Rice, Phys. Rev. B **18**, 2840 (1978); K. Takayama and M. Oka, Nucl. Phys. **A551**, 637 (1993); G. Mussardo, V. Riva, and G. Sotkov, Nucl.

Phys. **B699**, 545 (2004); G. Mussardo, V. Riva, G. Sotkov, and G. Delfino, Nucl. Phys. **B736**, 259 (2006).

[28] I. Nandori, S. Nagy, K. Sailer, and U. D. Jentschura, Nucl. Phys. **B725**, 467 (2005).

[29] J. Comellas, Nucl. Phys. **B509**, 662 (1998); M. E. Fisher, Rev. Mod. Phys. **70**, 653 (1998); C. Bagnuls and C Bervillier, Phys. Rep. **348**, 91 (2001); I. Nandori, K. Sailer, U. D. Jentschura, and G. Soff, J. Phys. G **28**, 607 (2002).

[30] N. Tetradis and C. Wetterich, Nucl. Phys. **B398**, 659 (1993); T. R. Morris, Int. J. Mod. Phys. A **9**, 2411 (1994); D. F. Litim, Phys. Lett. B **486**, 92 (2000); J. Alexandre and J. Polonyi, Ann. Phys. (N.Y.) **288**, 37 (2001); J. Berges, N. Tetradis, and C. Wetterich, Phys. Rep. **363**, 223 (2002); J. Polonyi, Central Eur. J. Phys. **1**, 1 (2003); J. Polonyi and K. Sailer, Phys. Rev. D **71**, 025010 (2005); J. M. Pawlowski, Ann. Phys. (N.Y.) **322**, 2831 (2007).

[31] A. Ringwald and C. Wetterich, Nucl. Phys. **B334**, 506 (1990); N. Tetradis and C. Wetterich, Nucl. Phys. **B383**, 197 (1992).

[32] I. Nandori and K. Sailer, Philos. Mag. **86**, 2033 (2006).

[33] I. Nandori, J. Phys. A **39**, 8119 (2006); U. D. Jentschura, I. Nandori, and J. Zinn-Justin, Ann. Phys. (N.Y.) **321**, 2647 (2006).